Drifting subpulse phenomenon in pulsars

Lofar perspective

Janusz Gil

J. Kepler Astronomical Institute
University of Zielona Góra,
Poland

Collaborators:

G. Melikidze, B. Zhang, U. Geppert, F. Haberl, J. Kijak, M. Sendyk

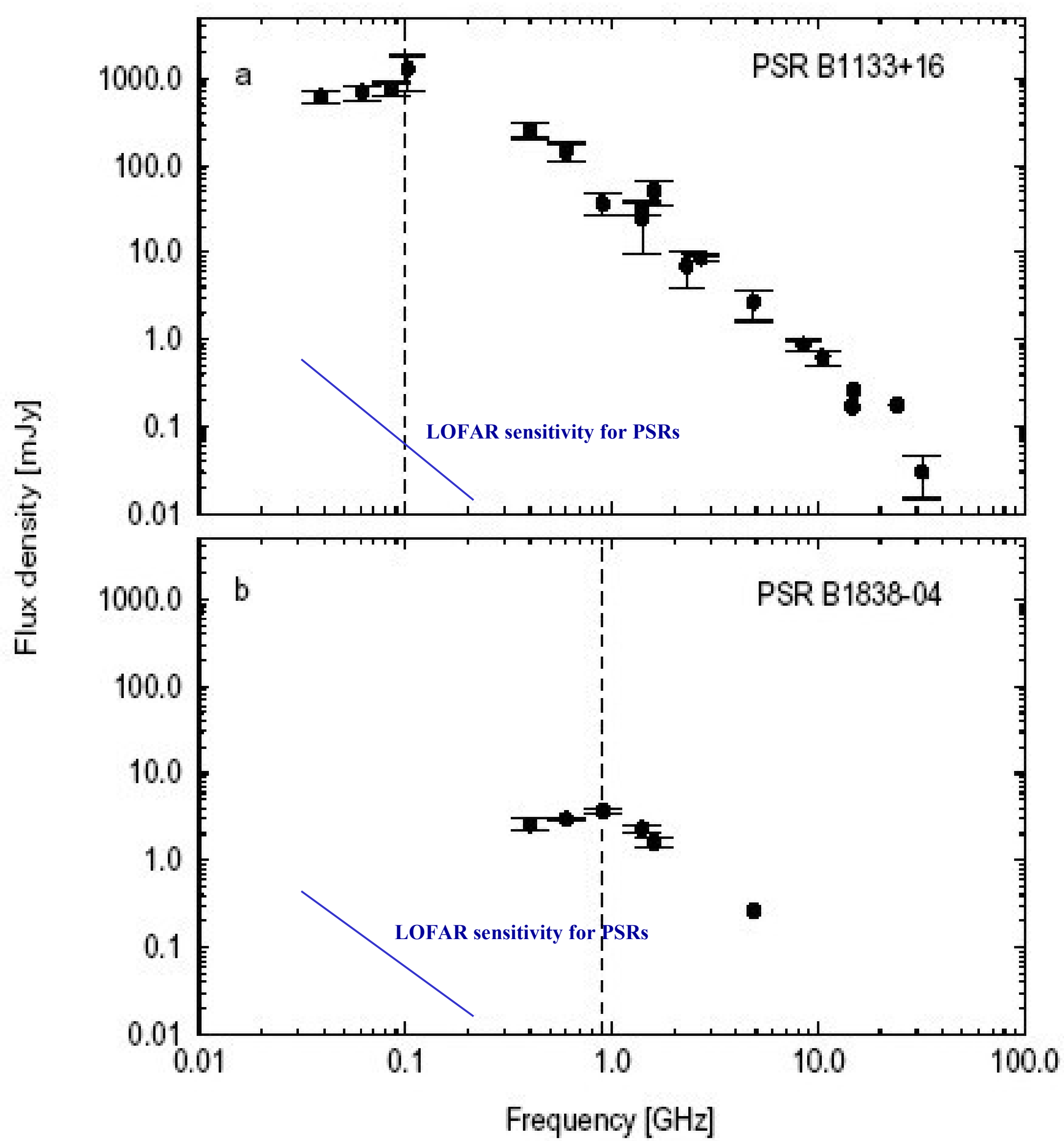

a
PSR B1133+16
b
PSR B1838-04
LOFAR sensitivity for PSRs
LOFAR sensitivity for PSRs
Flux density [mJy]
1000.0
100.0
10.0
1.0
0.1
0.01
0.01
0.1
1.0
10.0
100.0
Frequency [GHz]

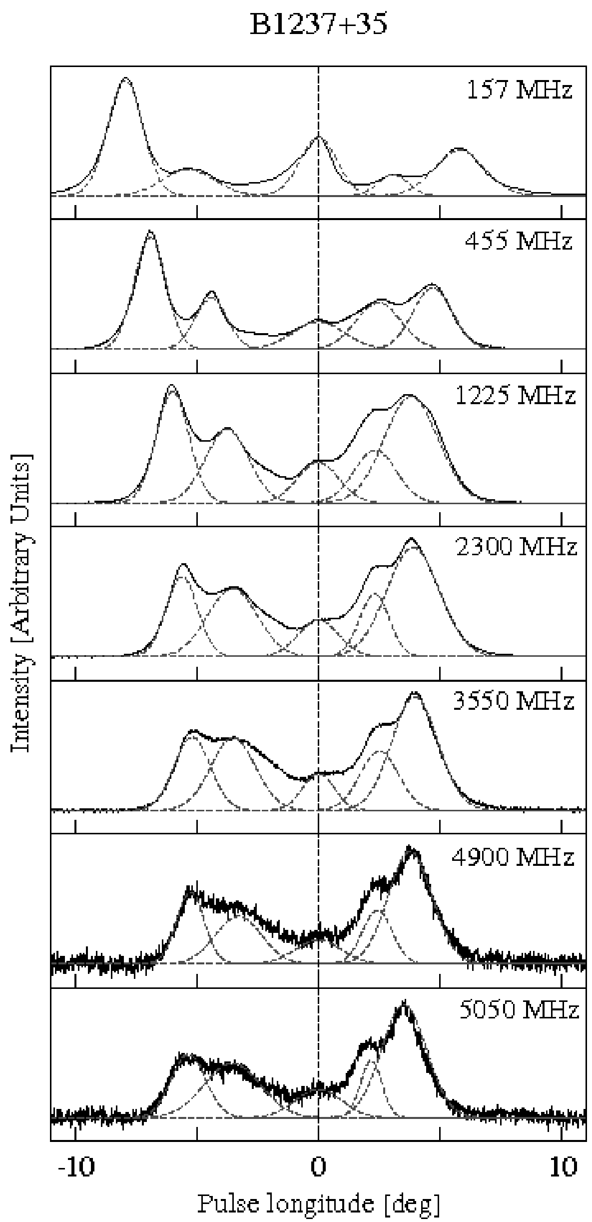

Broadening of the profile As frequency decreases

Evidence of the radius-to-frequency mapping and dipolar nature of magentic field lines in the emission region

Sensitive observations below 160 MHz would be highly desirable

40 years after discovery of pulsars the actual mechanism of their coherent radio emission is still a mystery.

Drifting subpulses, which seem to be a common phenomenon in pulsar radiation, is also a puzzle.

„The mechanism for drifting subpulses cannot be very different from the mechanism of observed radio emission ...

...intrinsic property of radiation mechanism „

(Weltevrede, Edwards & Stappers 2006, A&A 445,243)

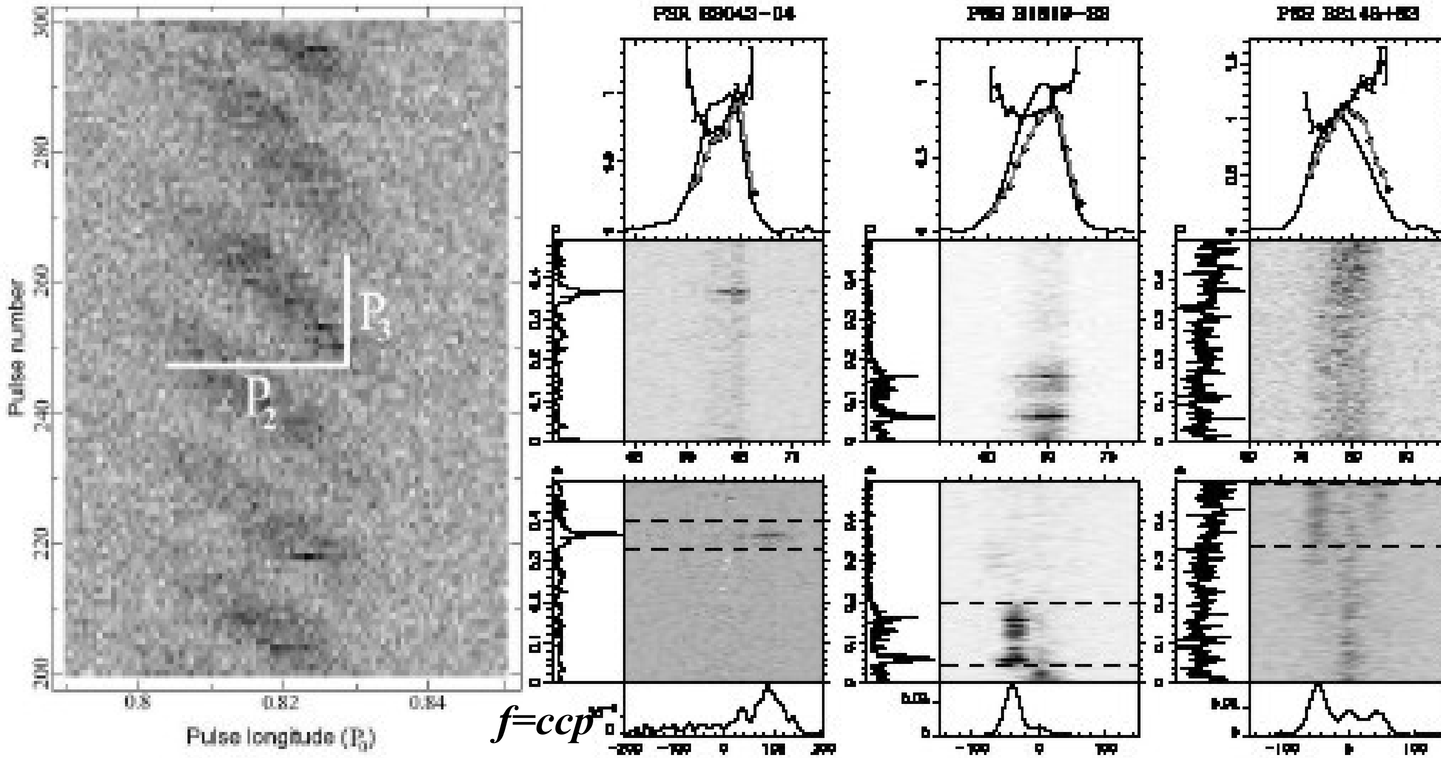

Fig. 1. The left panel shows a pulse-stack of one hundred successive pulses of PSR B1819−22. Two successive drift bands are vertically separated by P_3 and horizontally by P_2. The products of our analysis are shown for three pulsars. The top panel shows the integrated pulse profile (solid line), the longitude-resolved modulation index (solid line with error bars) and the longitude-resolved standard deviation (open circles). Below this panel the LRFS is shown with on its horizontal axis the pulse longitude in degrees, which is also the scale for the abscissa of the plot above. Below the LRFS the 2DFS is plotted and the power in the 2DFS is vertically integrated between the dashed lines, producing the bottom plots. Both the LRFS and 2DFS are horizontally integrated, producing the side-panels of the spectra. See the main text for further details about the plots.

$$P_2 = \pm P / cpp$$

LRFS - Longitude Resolved Fluctuation Spectrum

2DFS - Two Dimensional Fluctuation Spectrum – calulated along various slopes

Unbiased search for drifting subpulses in 187 (191) pulsars

About 55 % (more) of drifting subpulse pulsars

Weltevrede, Edwards & Stappers et al. 2006, 2007

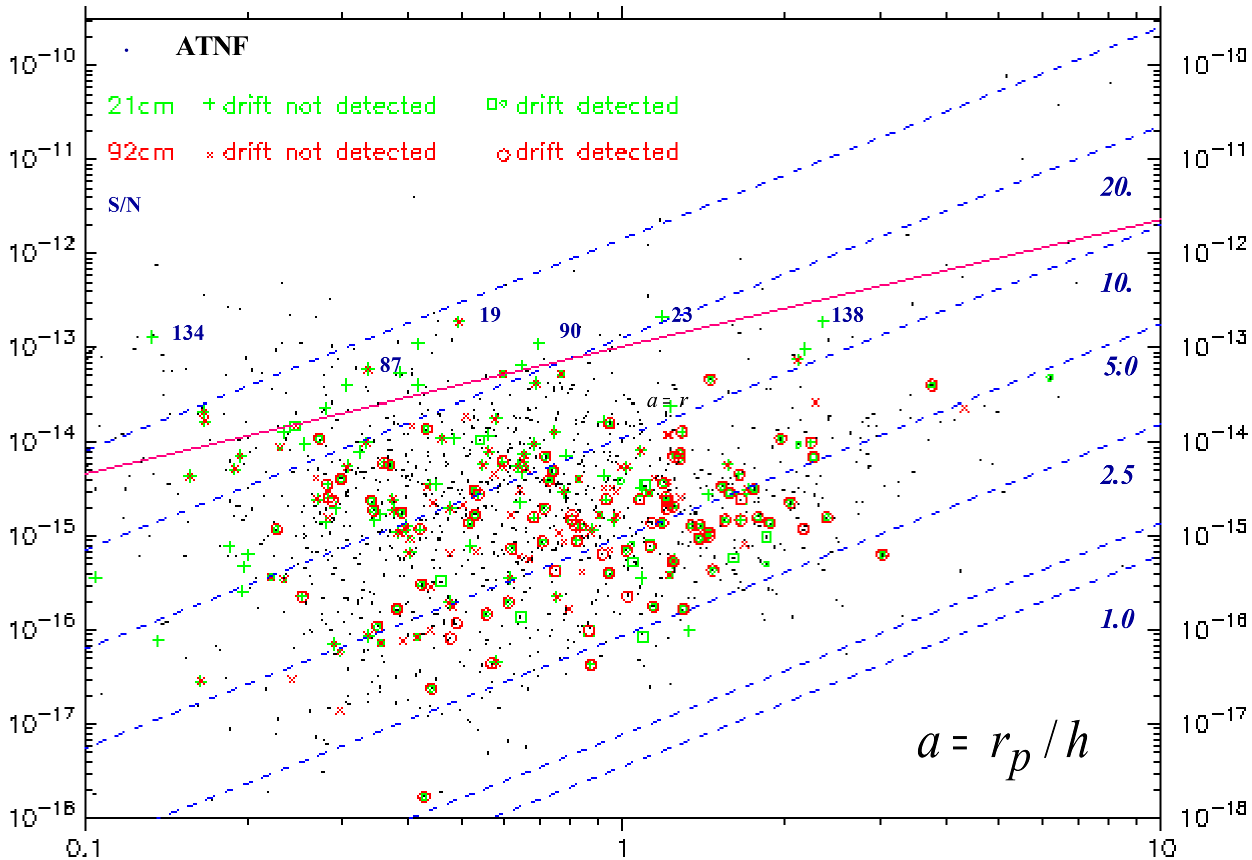

At frequencies lower than 320 MHz (LOFAR range) the ratio of detected drifting subpulses should be even higher

$D \approx d \approx h$

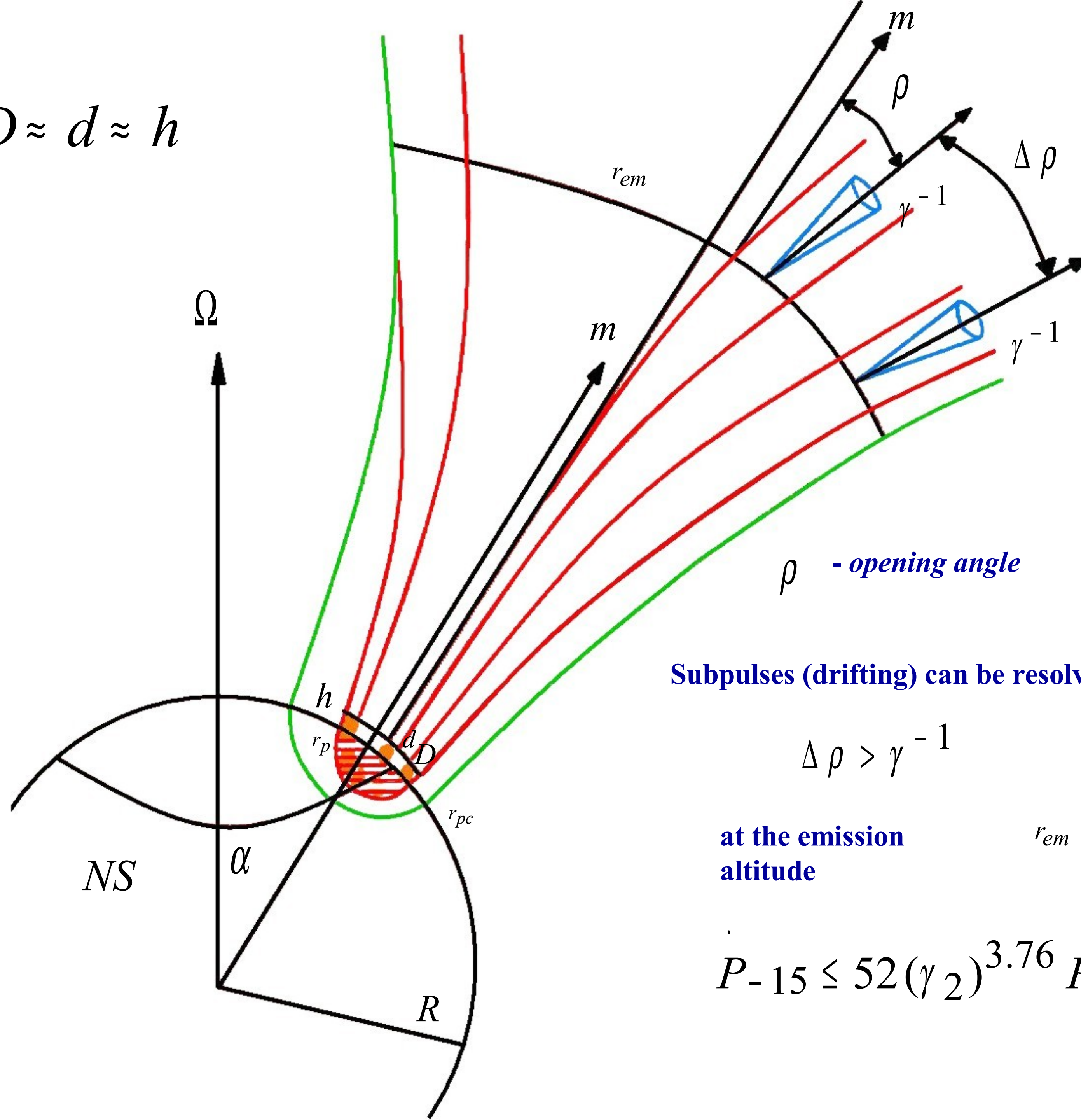

ρ **- *opening angle***

Subpulses (drifting) can be resolved if

$$\Delta \rho > \gamma^{-1}$$

at the emission altitude r_{em}

$$\dot{P}_{-15} \leq 52(\gamma_2)^{3.76} P^{1.35}$$

Unbiased search for drifting subpulses in 187 (191) pulsars

About 55 % (more) of drifting subpulse pulsars

Weltevrede et al. 2006, 2007

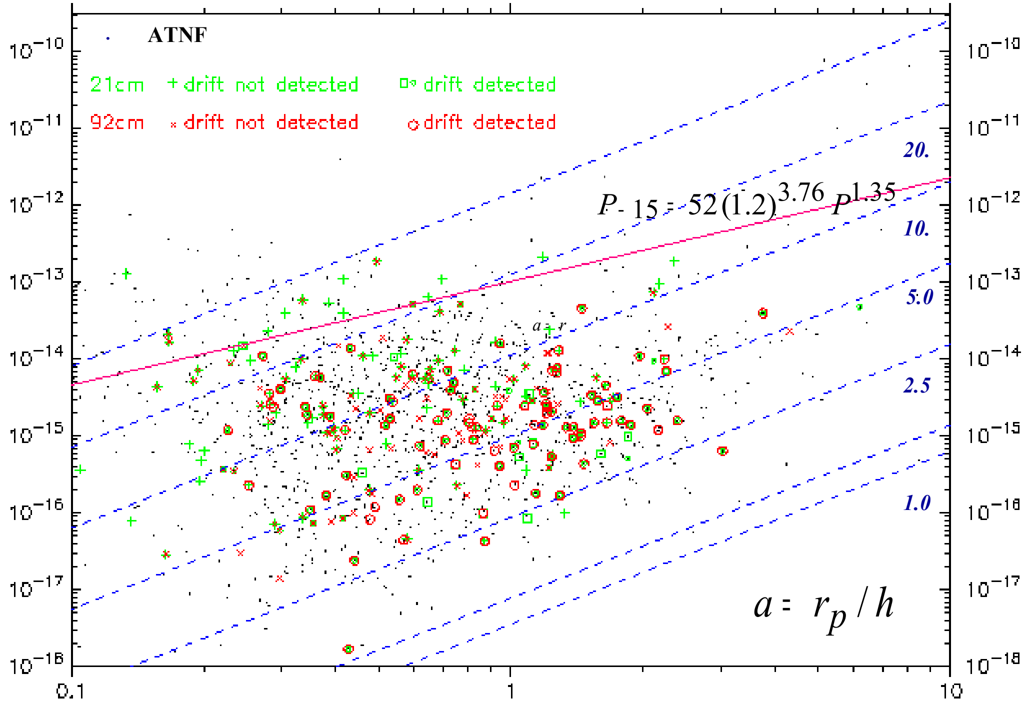

Lorentz factor

$\gamma = 120$

Carousel model

Sub-beams of radio emission presumably related to sparks operating just above the Polar Cap circulate around the magnetic axis

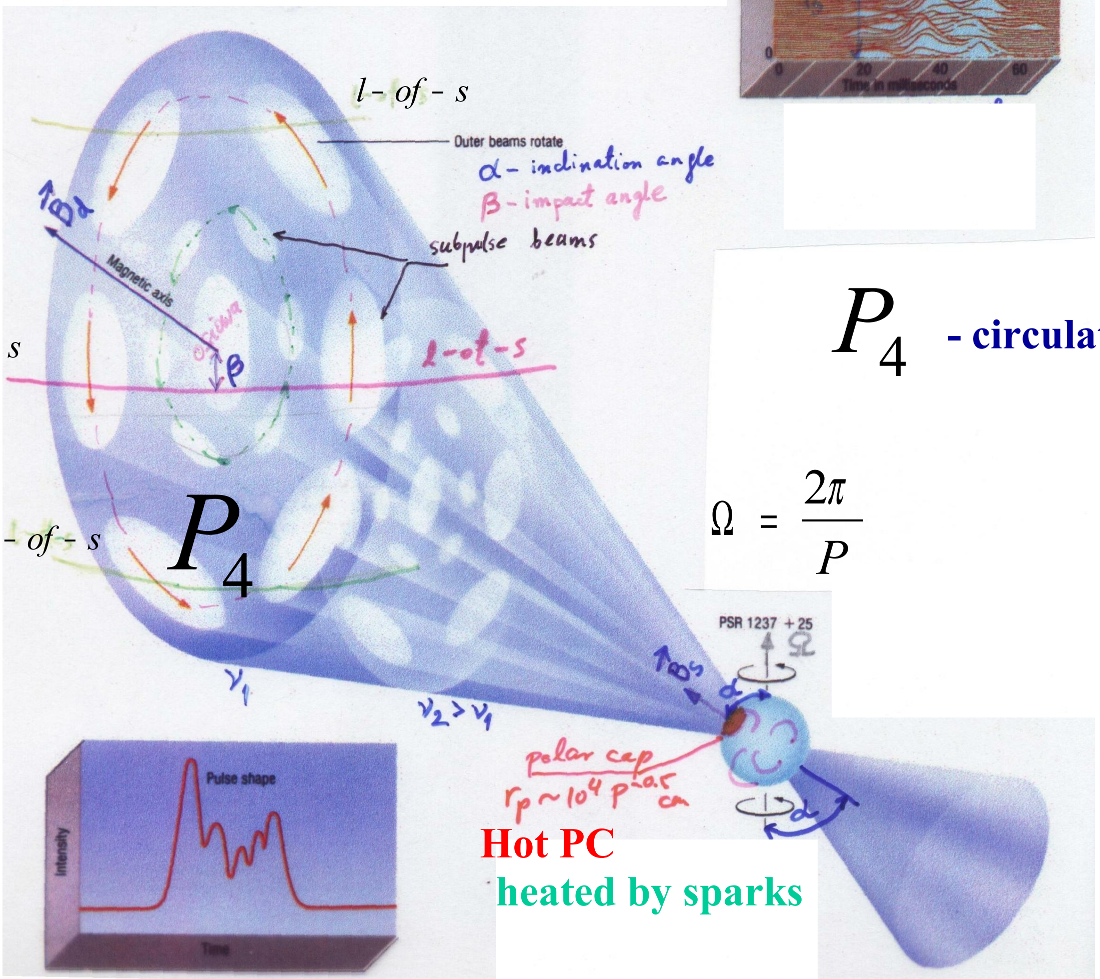

Hot PC
heated by sparks

$$\Omega = \frac{2\pi}{P}$$

P_4 - circulational periodicity ?

Subpulse drift

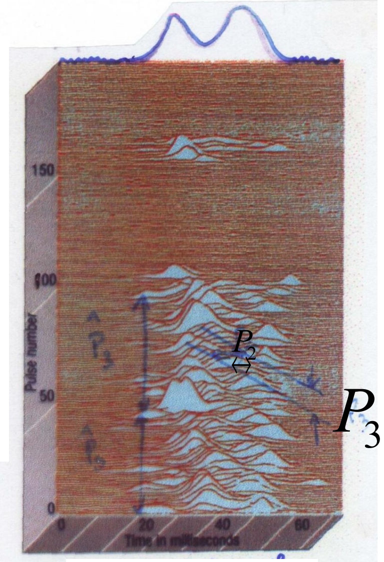

Subpulses in subsequent pulses arrive in phases determined by the apparent drift rate

$$D = P_2 / P_3$$

Polar cap

$$r_{pc} = 1.45 \times 10^4 P^{-0.5}\, cm$$

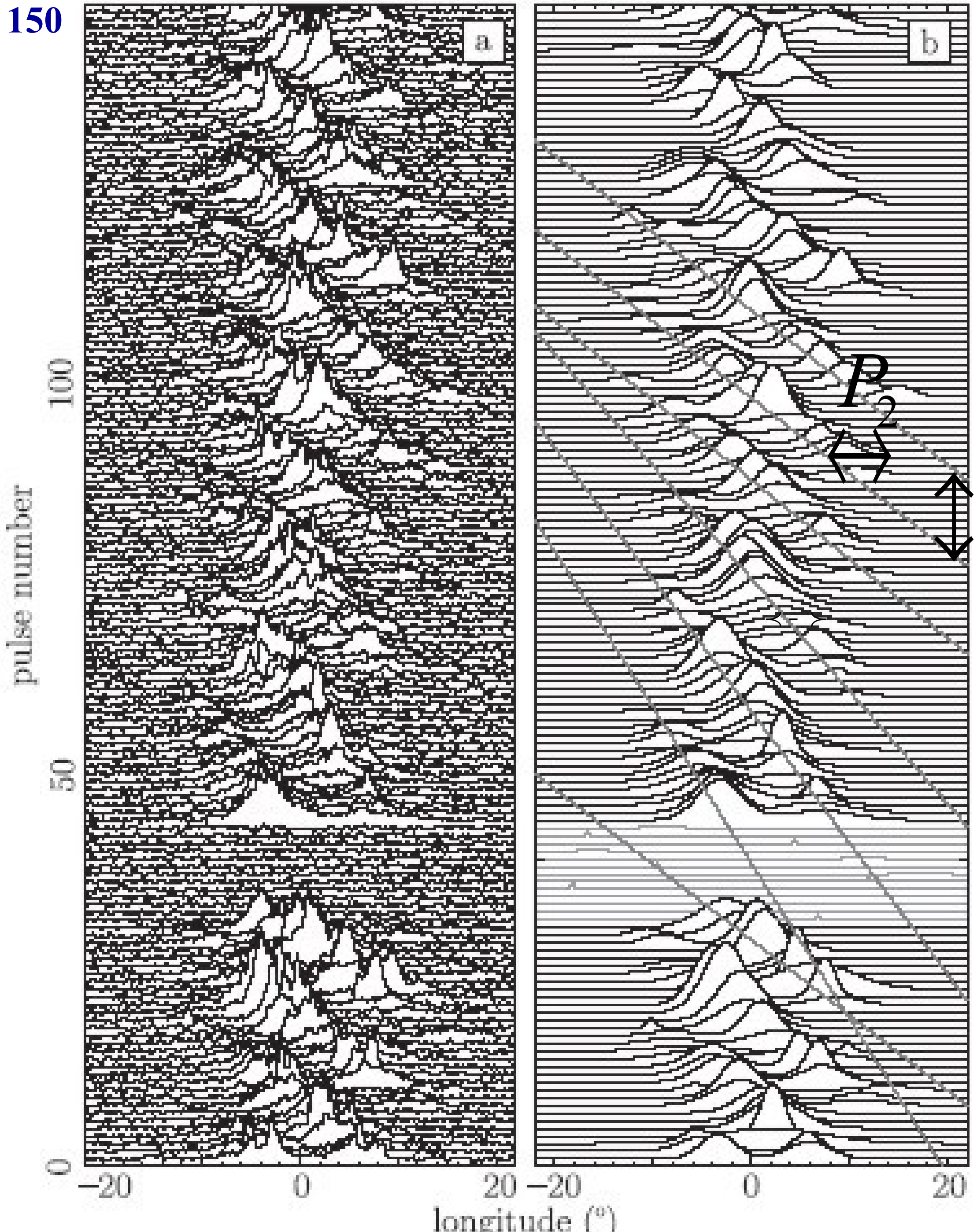

PSR B0809+74

Perhaps the best example of
Drifting subpulses
phenomenon in pulsars

Apparent subpulse drift-bands

$P_3 \approx 11P$

Modulation of intensity along drift-bands consistent with carousel model

that is

Sub-beams continue
to circulate beyond
the observed pulse-window

(after van Leuven, Stappers et al..)

B0818-41

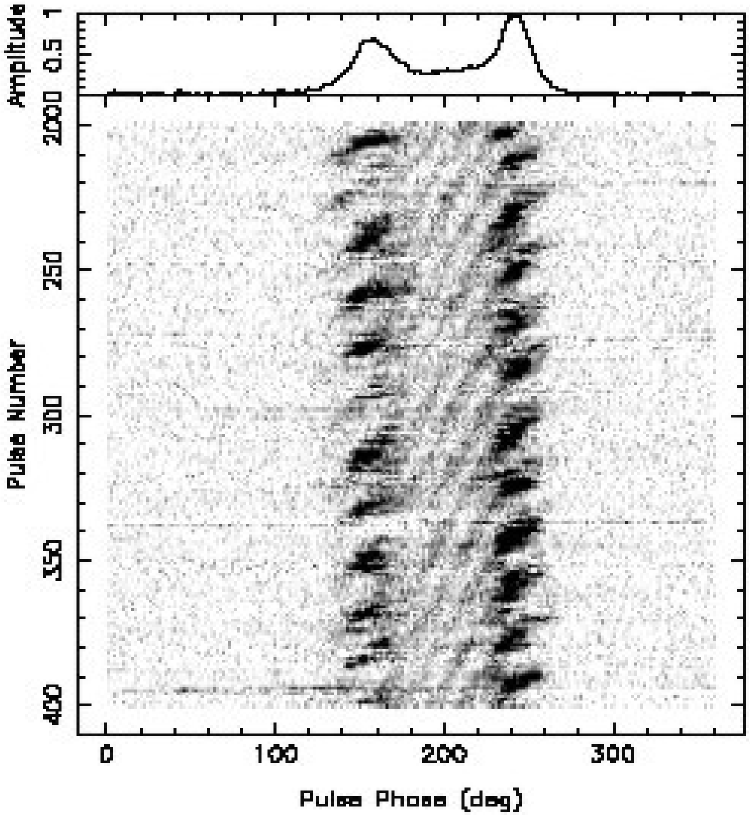

Figure 2. Grey-scale plot of single-pulse data (pulse # 200 to 400) of PSR B0818−41 at 325 MHz, with the average profile shown on top. Signatures of radio frequency interference are present around pulse numbers 220, 298, 338 and 397.

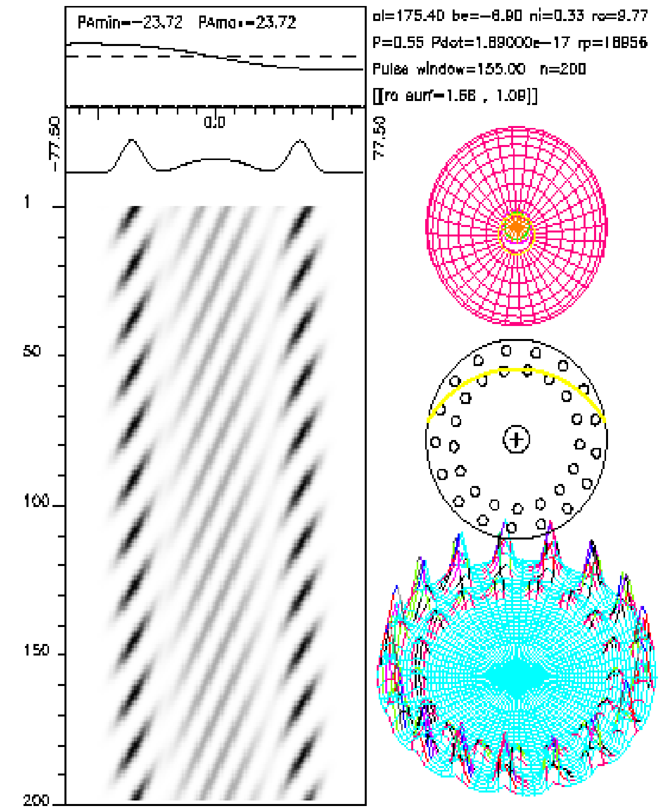

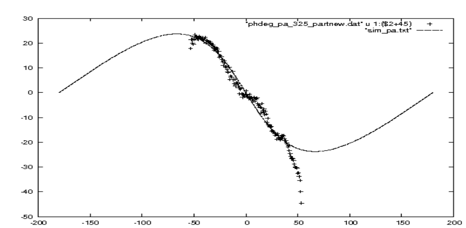

$\alpha = 175^{\circ}$

$\beta = 7^{\circ}$

PSR B 0818-41

LRFS

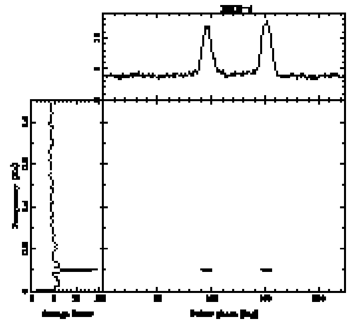

Figure 17: The contour plot of the power spectrum of the flux at 225 MHz as a function of phase (longitude) during a sequence of 200 pulses (pulse # 200–400). The left panel shows the power spectrum integrated over longitude. The upper panel shows the power integrated over frequency.

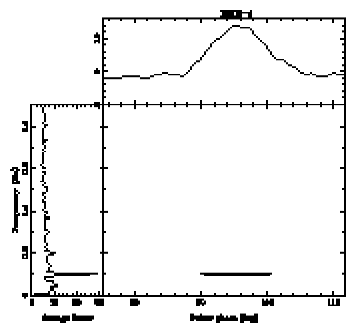

Figure 18: The contour plot of the power spectrum of the flux at 225 MHz as a function of phase (longitude) during a sequence of 200 pulses (pulse # 200–400), for the component 1 (bin number 89–122). The left panel shows the power spectrum integrated over longitude. The upper panel shows the power integrated over frequency.

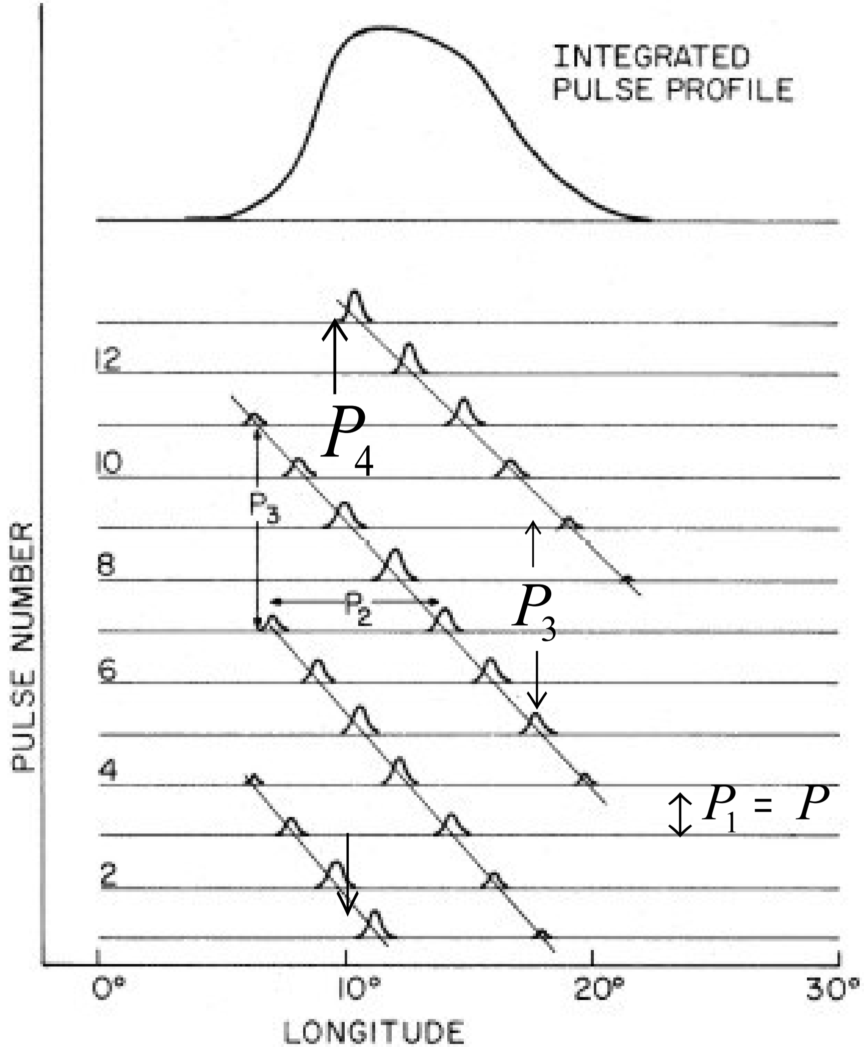

FIG. 5.—Schematic (after Backer 1973) of integrated pulse profile, arrival times of individual pulses, and definition of P_2, P_3 for those pulsars showing the "drifting subpulse" phenomenon. Arrival times of individual pulses are given in terms of a longitude for which 360° corresponds to the full pulsar period.

Ruderman & Sutherland 1975

P_1, P_2, P_3, P_4

Apparent drift rate $D = P_2 / P_3$

P_2 **distance between driftbands in longitude**

P_3 **distance between driftbands in** P_1

Intrinsic drift rate $P_4 = P_3 N$

N **number of rotating sub-beams**

P_4 **distance between the same driftbands**

P_4 **time interval to complete one rotation around the pole**

very difficult to measure, only 8 cases known !!!

PSR B0943+10

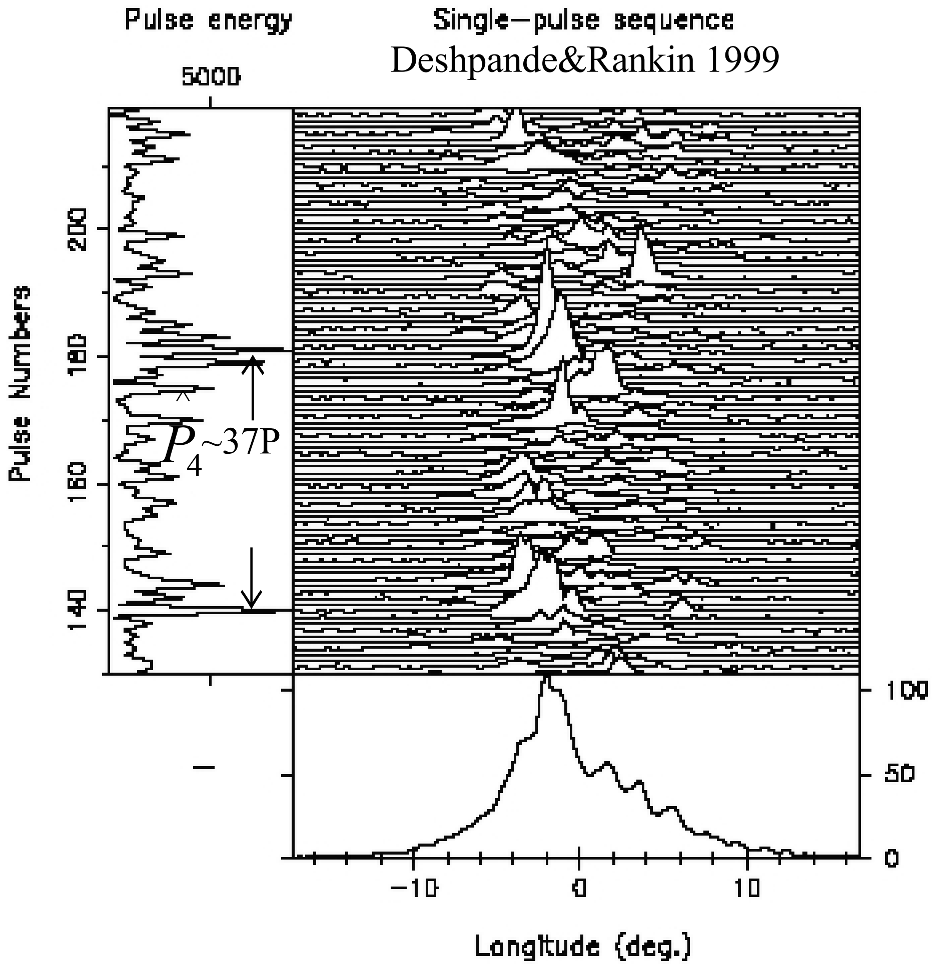

P=1.089 s

$P_3 = 1.87P$

$P_4 = 37.35P$

Number of sub-beams circulating around B

$N = P_4 / P_3 = 20$

PSR B0943+10

35 MHz observations
Asgekar & Deshpande 2001 f_4

430 MHz observations
Deshpande & Rankin f_3

Phased-resolved fluctuation spectrum

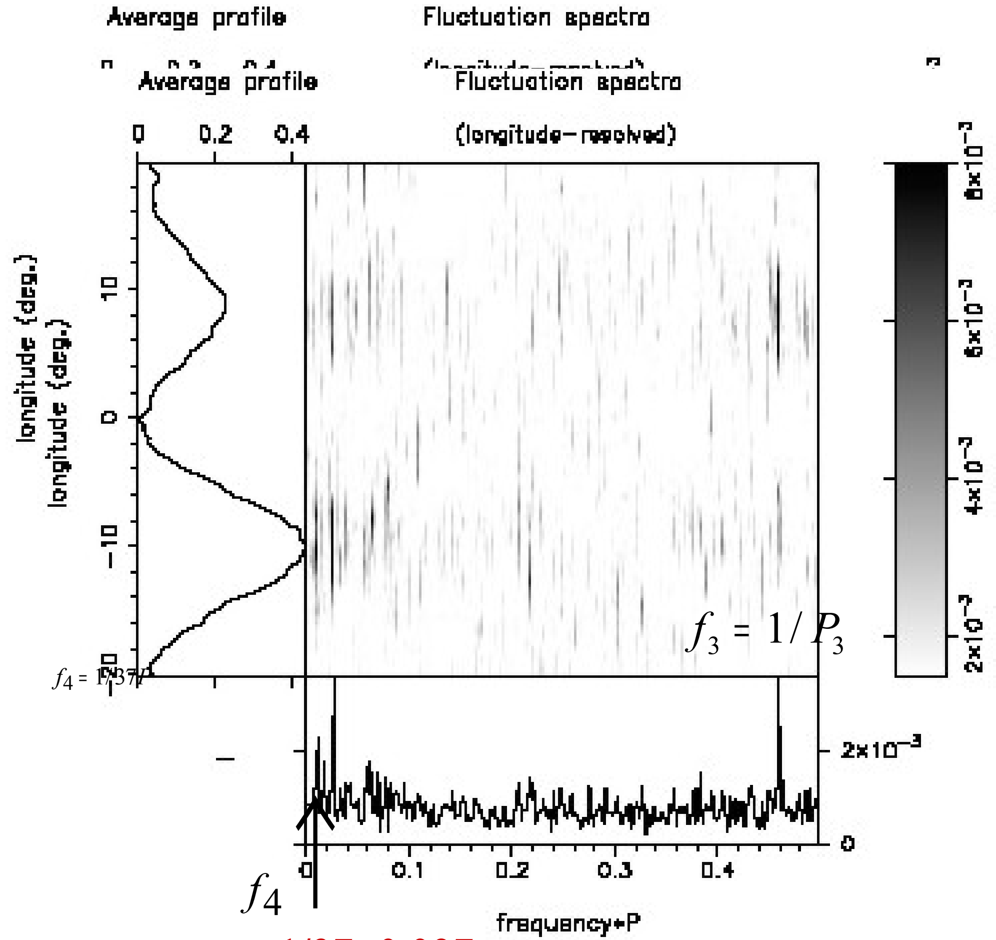

1/37=0.027

$$P_4 = 37.35\,P = 41\text{s.}$$

$$N = P_4 / P_3 = \frac{37.35}{1.87} = 20$$

Spectral analysis fully consistent with „carousel model”. Sub-beams continue to circulate around the beam axis beyond the pulse-window and reapear after the period needed to complete one full circulation around the magnetic axis

Low frequency observations (LOFAR range) are more sensitive to low frequency modulations possibly related to the „carousel” circulation times

Radius-to-frequency mapping

Frequency dependent beam size

PSR B0943+10

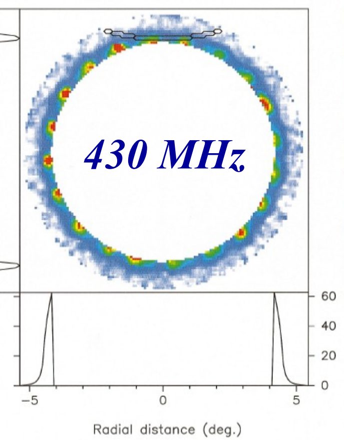

Arecibo

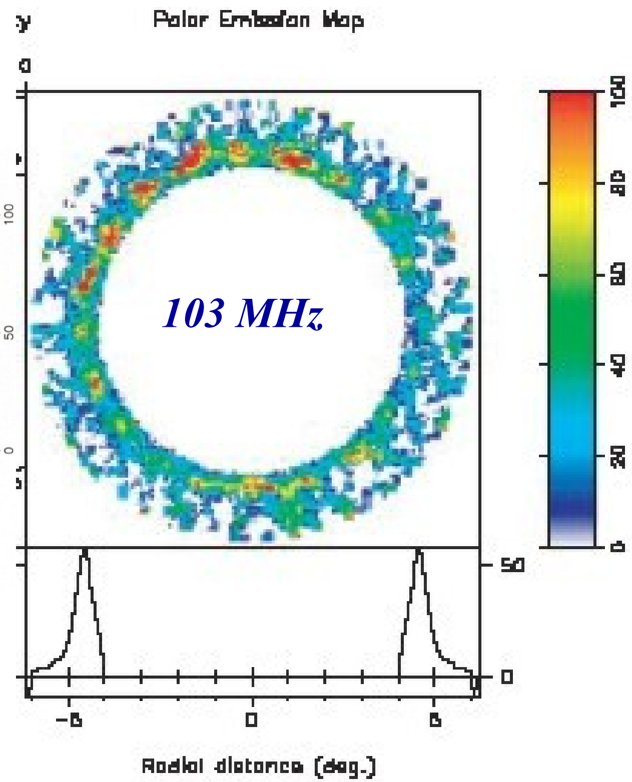

PRAO

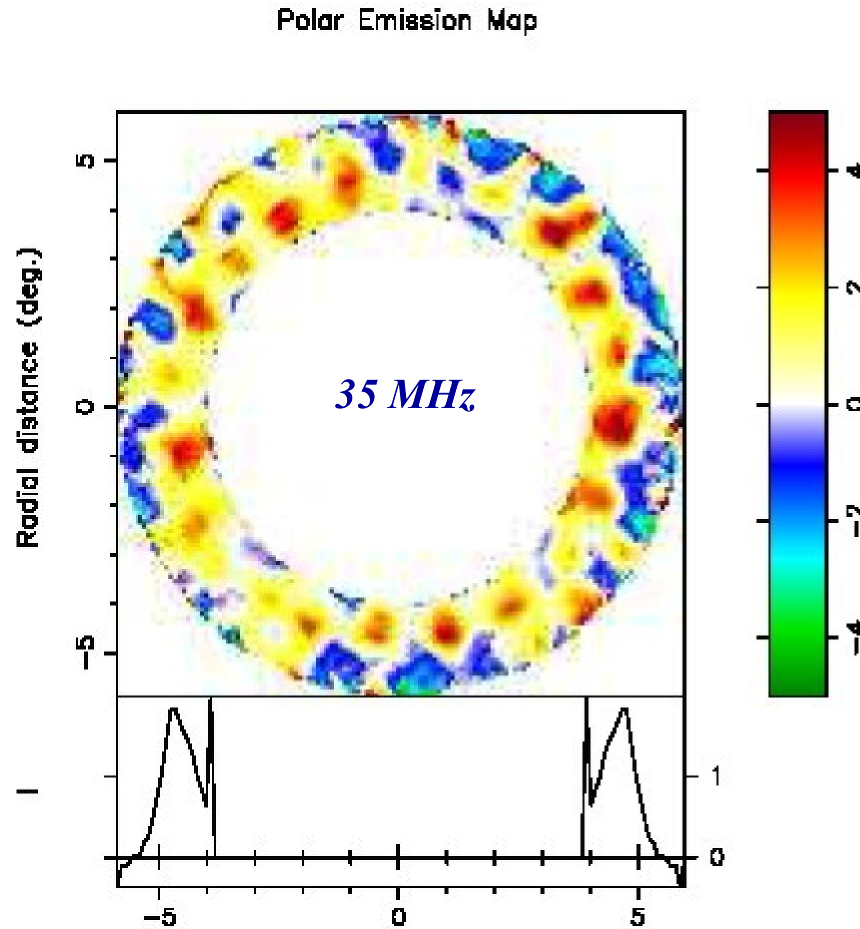

Gauribidanur

B1133+16

Arecibo 327 MHz

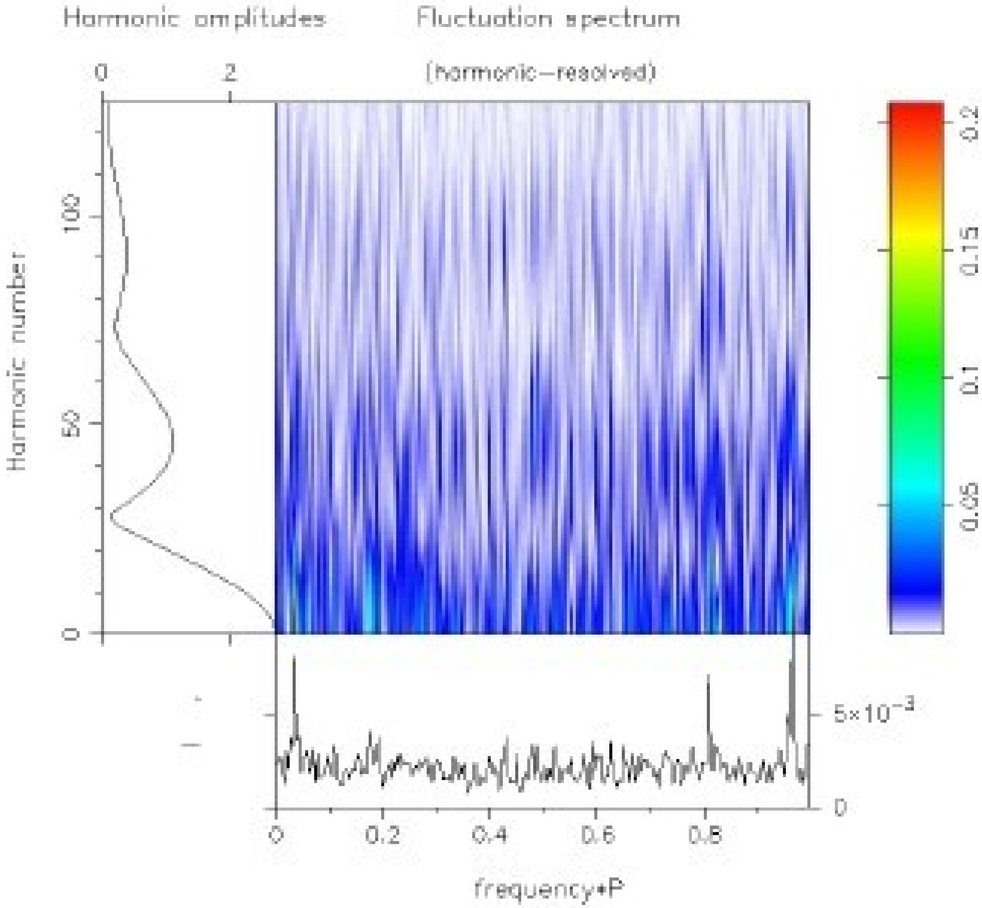

Rankin et al. 2007

B1133+16

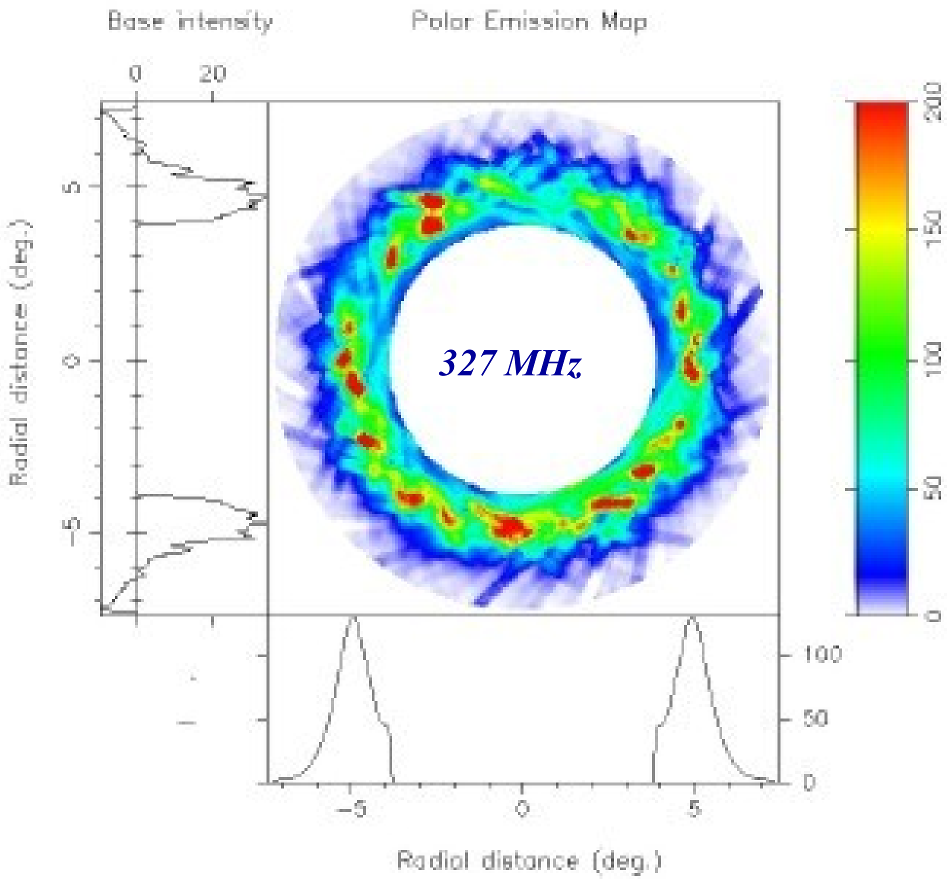

$P = 1.19 s$

$\dot{P}_{-15} = 3.7$

$\dot{E} = 9 \cdot 10^{31}\, erg/s$

$P_3 = 1.237\, P$

$P_4 = 28.44\, P$

$N = P_4 / P_3 = 22$

Arecibo Observatory

327 MHz

Rankin et al. 2007

B0943+10 Cartographic map of 20 subpulse beams „circulating" around the pole in about 37 pulsar periods

Deshpande & Rankin, 1999

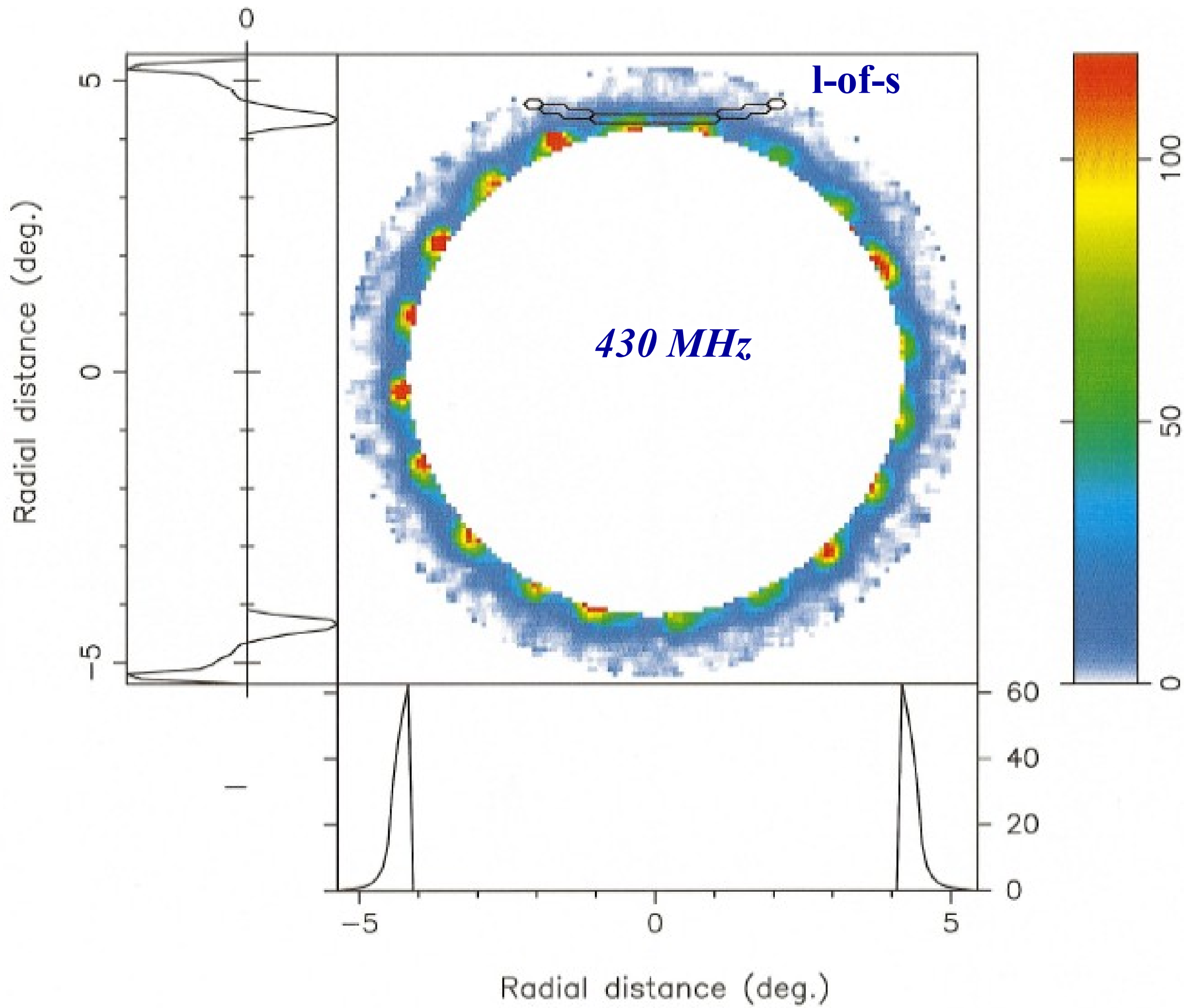

$P = 1.098$ s

$\dot{P}_{-15} = 3.52$

$\dot{E} = 10^{32}\ erg/s$

$P_3 = 1.86\ P$

$P_4 = 37.35\ P$

$N = P_4 / P_3 = 20$

α, β *Pulsar geometry known*

(Intensity; pulse longitude and pulse number) →(Intensity; polar colatitude and azimuth)

Clear manifestation of subpulse sub-beams circulating around the magnetic axis

B0943+10 430 MHz

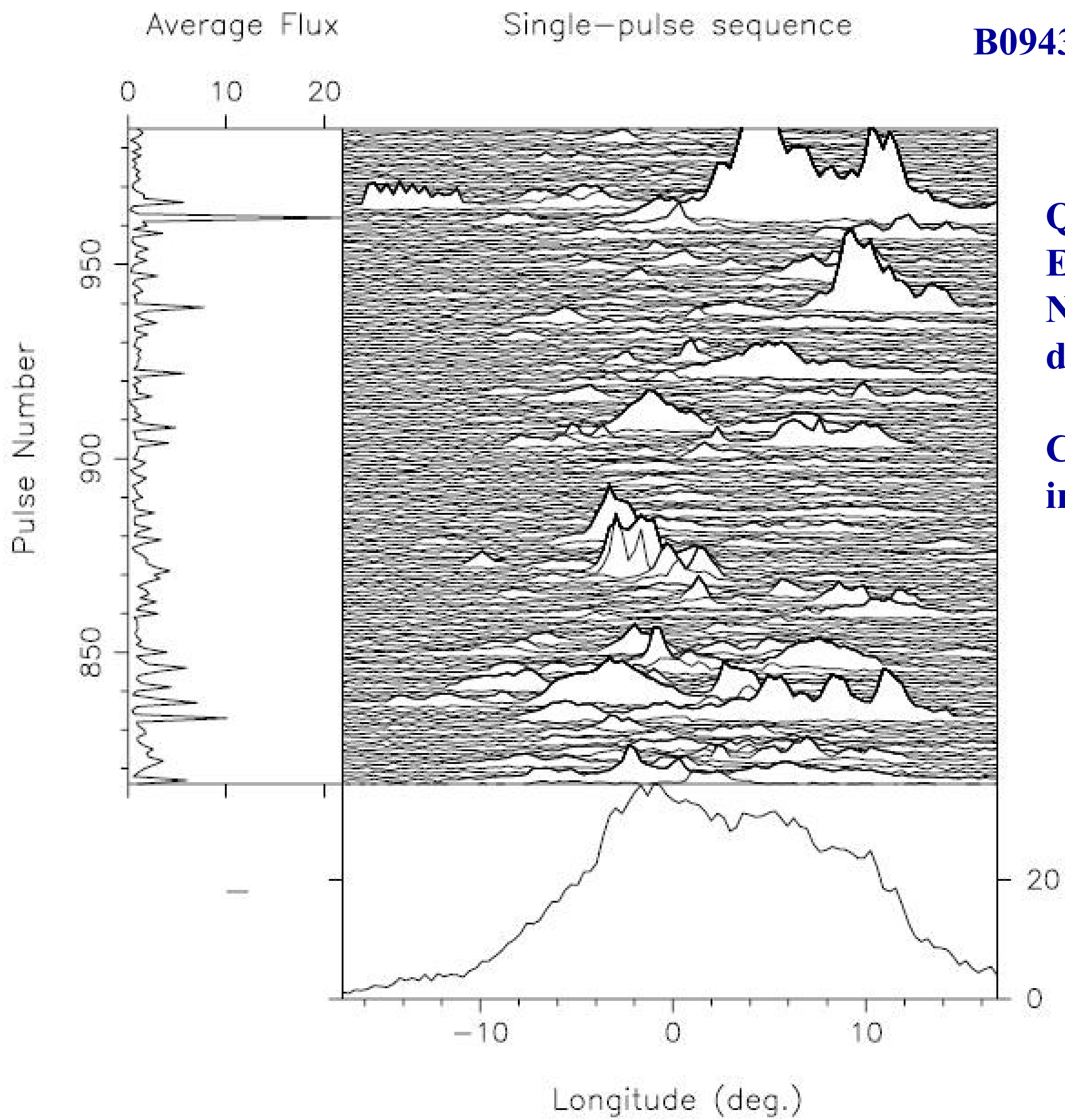

Q-mode
Erratic
No organized drift visible

Cartographic map impossible to make

103 MHz

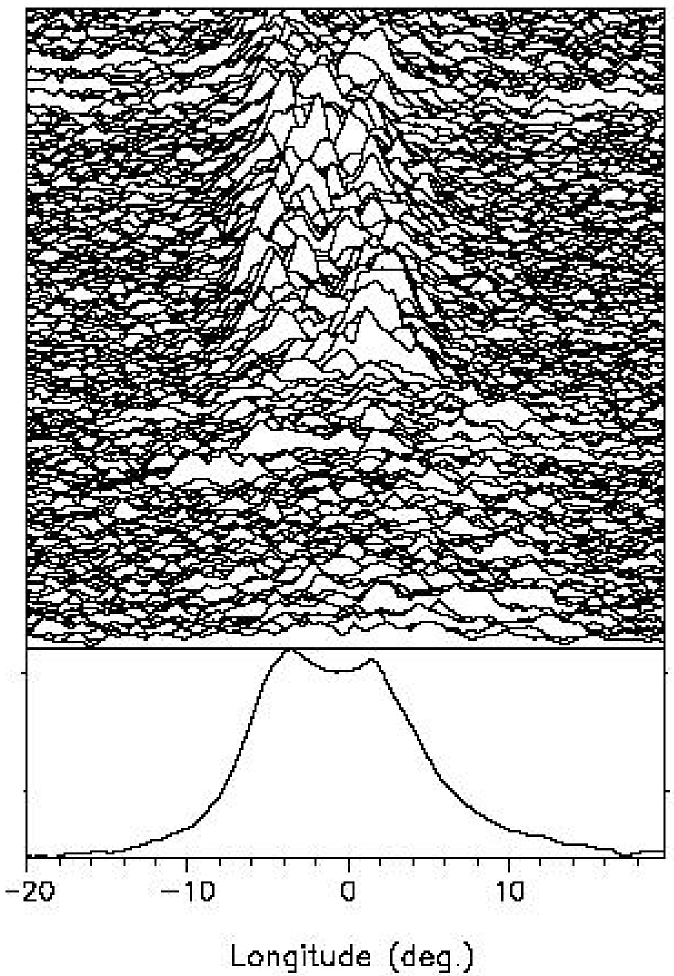

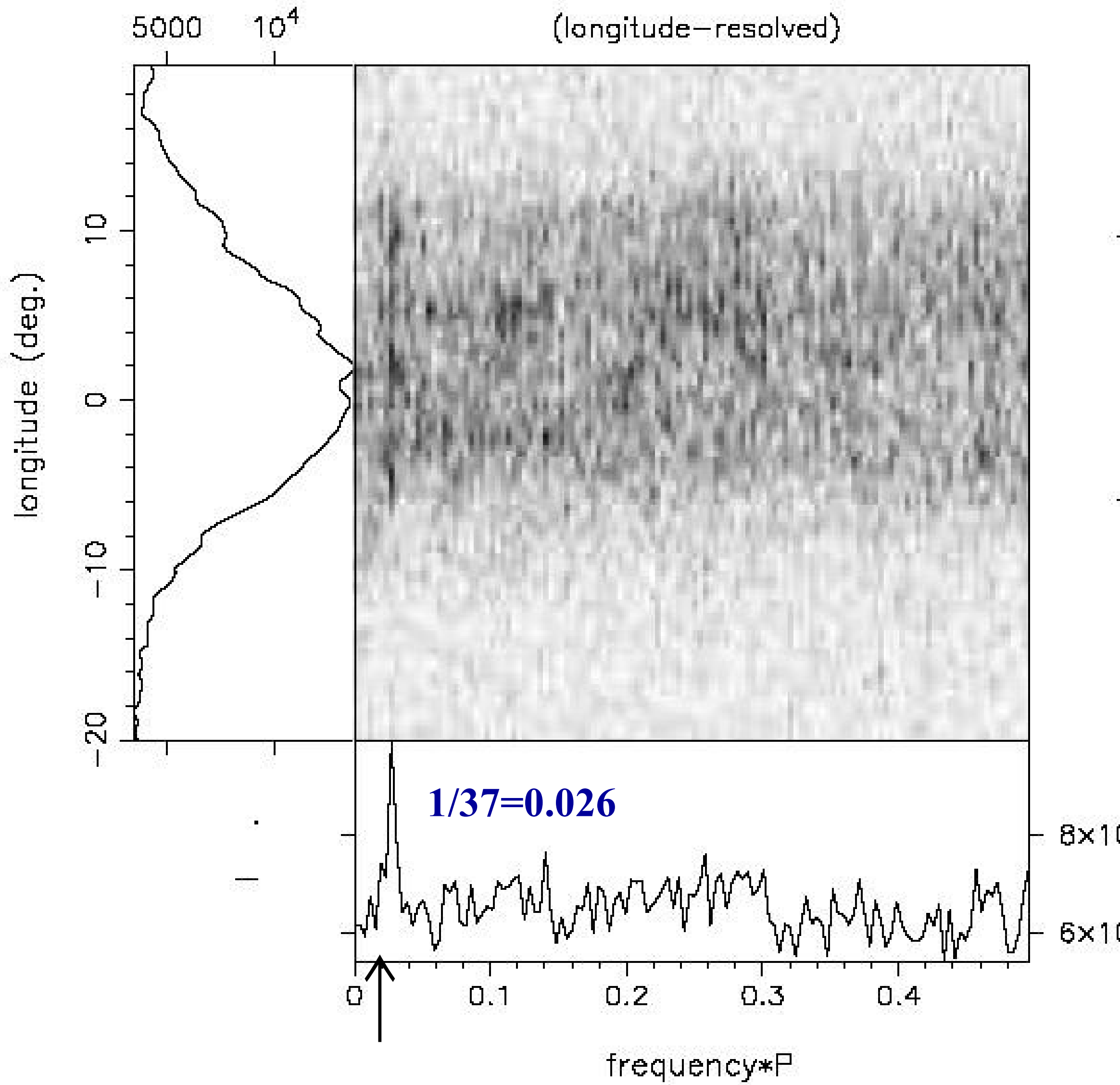

B0943+10 Q-mode (erratic)

Suleymanova & Rankin 2006

Clear feature at 37 P as in the B-mode

Spark plasma circulates around the local magnetic pole on the Polar Cap with a specific period P_4, regardless it is fragmented into equally spaced filaments or operates in much less organized manner.

One cannot swich off the E x B drift, except when there is no E or B.

Natural mechanism of subpulse drift

$E \times B$

Natural state of the magnetospheric plasma frozen into electric and magnetic field is corotation with NS (global corotation)

$$v_{cor} = c(E_c \times B_s)/B^2 = cE_c/B_s \quad \Leftarrow \quad \rho = \rho_{GJ}$$

corotation

$$if \quad E \neq E_c \quad then \quad v \neq v_{cor} \quad \Leftarrow \quad \rho \neq \rho_{GJ}$$

Polar Gap charge depletion

Non-corotation plasma lags behind pulsar rotation and drifts with respects the polar cap surface with velocity v_{dr}

$$v_{dr} = c(\Delta E \times B_s)/B^2 = c\Delta E / B_s$$

ΔE Electric field associated with charge depletion $\Delta\rho = \rho_{GJ} - \rho$

If plasma has transversal structure (spark filaments) then this inevitable

$\Delta E \times B$ **drift should be observed in the form of drifting subpulses, and/or specific features in the intensity fluctuation spectrum**

$\overrightarrow{\Delta E} \times \vec{B}$ spark plasma circulation drift rate

Linear velocity of the E x B drift (RS75)

$$v_d = \frac{c\Delta E}{B_s} = \frac{c\eta\,(2\pi/cP)B_s h}{B_s} = \eta\,\frac{2\pi}{P}h \ \text{[cm/s]}$$

B_s *-actual surface magnetic field*
B_d *-dipolar magnetic field at PC*

ΔE *- component of electric field caused by charge depletion* $\Delta\rho = \rho_{GJ} - \rho_{th} = \eta\rho_{GJ}$

$$\omega = v_d/d = \eta\,(2\pi/P)(h/d)$$

Carusel angular speed

Time interval to complete one circulation around periphery of PC

$$P_4 = \frac{P}{2\eta}\frac{d}{h} \le \frac{P}{2\eta}\frac{r_p}{h}$$

Gil, Melikidze & Geppert 2003

Within the model of the inner acceleration region to surface of the PC is heated to high temperatures by the back-flow of particles produced in sparking discharges.

The heating rate is determined by the same value of the electric field that is involved in the E x B drifting phenomenon.

thus, the observed drifting rate

$$P_4 = 2\pi\ d / \upsilon_d = \frac{P}{2\eta}\frac{d}{h} \leq \frac{P}{2\eta}\frac{r_p}{h}$$

and the observed heating rate (thermal X-ray luminosity from hot PC)

$$L_x = \sigma T_s^4 A_{bol} = \sigma T_s^4 A_{pc} (B_d / B_s)$$

should be strongly correlated.

Thermal X-ray luminosity from spark-heated polar cap

$$L_x = 2.5 \times 10^{31} \times (\dot{P}_{-15} / P^3)(P_4 / P)^{-2} \quad \textit{\textbf{erg/s}}$$

Efficiency

$$\dot{E} = I\Omega\dot{\Omega}$$

Spin-down power

$$L_x / \dot{E} = (0.63 / I_{45})(P_4 / P)^{-2}$$

$$I = I_{45} 10^{45}\ g\,cm^2$$

$$I_{45} = 1 \pm 0.15$$

.

X-ray Multi Mirror (XMM) – Newton satelite telescope

One revolution on an excentric orbit around the Earth takes 48 hours – observations are not performed close to the Earth due to strong noise contamination

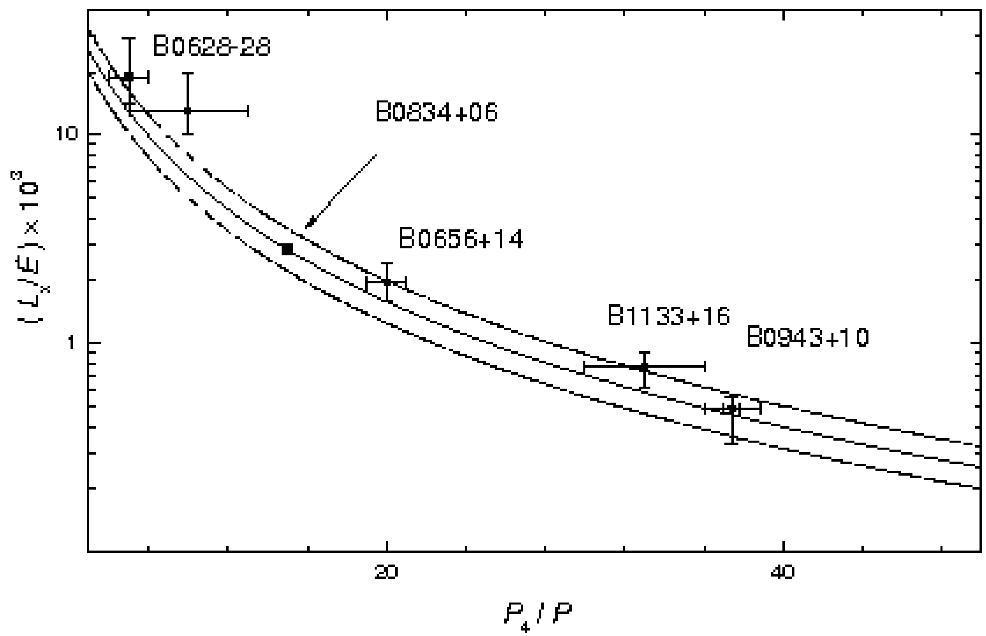

$I_{45} = 1 \pm 0.15$

$$L_x/\dot{E} = (0.63/I_{45})(P_4/P)^{-2}$$

Further low frequency LOFAR observation using 2DFS techniques should result in

Detection more drifting subpulse pulsars and pussible more determination of P_4

In nearby pulsars, in which thermal X-ray component from hot polar cap can be determined. Then the polar gap relationship $L_x \propto P_4^{-2}$ **can be tested further.**

B0628-28   L_x=2.78 x 10^30 erg/s   E_dot=1.5 x 10^32 erg/s ➔ P_4=6 P

Weltevrede et al..2006   P_3=(7+/-1) P ➔ P_4=P_3

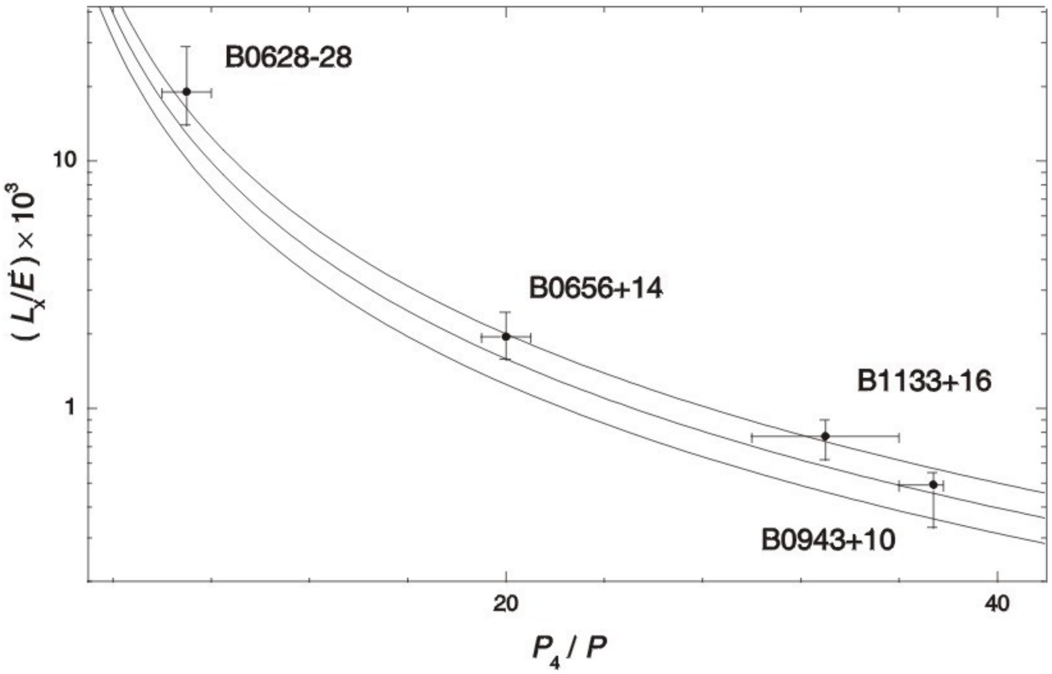

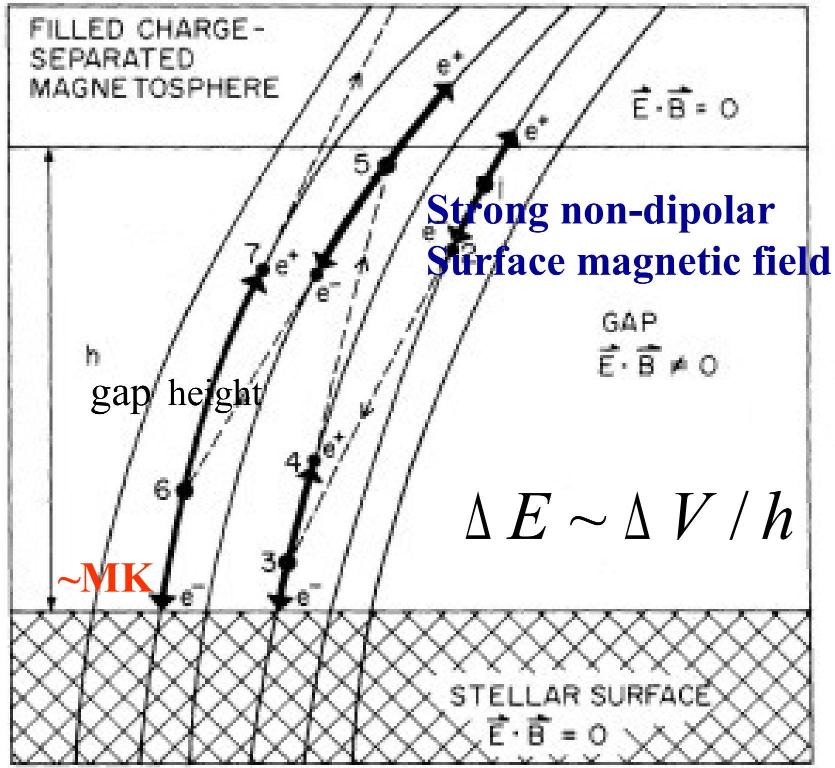

Within the acceleration region the spark generated positrons are moving towards the magnetosphere while back-flow of electrons bombard the polar cap surface and heat it to MK temperatures

Ruderman & Sutherland 1975

Pure vacuum gap

Charge depletion maximum possible $\Delta\rho = \rho_{GJ}$

Very strong electric field ΔE

$\Delta E \times B$ **drift much too fast as compared with observations**

Polar cap heating too intense and subpulse drift was too fast as compared with observations

Modification needed

Future work

New XMM-Newton observations of PSR B0826-34
50 Ks performed in November 2006
Zhang, Gil, Melikidze, Geppert, Haberl

Non-detected $P_4/P = 14 \pm 1$ **(Gupta, Gil, Kijak, Sendyk 2004)**

Proposal for XMM-Newton observations of
PSR B0834+06 accepted – observation in summer 2006
(simultaneous radio observations with GMRT planned)

Very promissing $P_4/P = 15 \pm 1$ **(Asgekar, Deshapande 2005)**

Proposal for XMM-Newton observations of PSR B1702-19
will be submitted for the next cycle

Very promissing $P_4/P = 10 \pm 1$ **(Weltevrede 2006; GMRT planned)**

Co-rotating magnetosphere

$$E_c = -(\Omega \times r/c) \times B_s$$

Force-free magnetosphere

$$E_c \cdot B_s = 0$$

$$\Delta V_{||} = 0$$

No acceleration along *B*

GJ69, RS75

$$\rho_c = (1/2\pi)\, divE_c =$$

$$= -\Omega \cdot B_s/(2\pi c) = \pm B_s/cP$$

Co-rotating charge density

$$v_{cor} = c(E_c \times B_s)/B^2 = cE_c/B_s$$

Linear co-rotation velocity

Name	$\hat{P}_3/P$		$L_x/\dot{E} \times 10^{-3}$		$L_x \times 10^{28}$		b	$T_s^{(obs)}$	$T_s^{(pred)}$	B_d	B_s
PSR B	Obs.	Pred.	Obs.	Pred.	Obs.	Pred.	A_{pc}/A_{bol}	10^6 K	10^6 K	10^{12}G	10^{14}G
$0943+10$	37.4	37	$0.5^{+0.2}_{-0.2}$	0.46	5^{+2}_{-2}	4.8	60^{+140}_{-48}	$3.1^{+0.9}_{-1.1}$	3^{+1}_{-1}	3.95	$2.37^{+5.53}_{-1.90}$
$1133+16$	(33^{+3})	31^{+3}	$0.77^{+0.13}$	$1.0^{+0.3}$	$7.7^{+1.3}$	$8.9^{+1.3}$	$11.1^{+16.6}$	$2.8^{+1.2}$	$2.4^{+0.8}$	4.25	$0.47^{+0.71}$

The only two cases existing with both measurements

B1133+16 $L_x/\dot{E} \sim 0.77 \times 10^{-3}$ $\hat{P}_3/P \sim 33$

B0943+10 $L_x/\dot{E} \sim 0.5 \times 10^{-3}$ $\hat{P}_3/P \sim 37$

Gil, Melikidze & Zhang 2006

$$\eta = (1/2\pi)(P/P_3)$$

Screening factor ~(0.05-0.1)

only few % of GJ plasma involved in acceleration

$$L_x = 2.9 \times 10^{31} \times (\dot{P}_{-15}/P^3)(\hat{P}_3/P)^{-2} \quad \text{erg/s}$$

X-ray bolometric luminosity

$10^{(28-29)}\ erg/s$

$$L_x/\dot{E} = 0.63(\hat{P}_3/P)^{-2}$$

Efficiency ~ 0.001

$$T_s = (8.2\times 10^6\ K)\ A_4^{-0.25}\ \dot{P}_{-15}^{\ 0.25}\ P^{-0.75}\ (\hat{P}_3/P)^{-0.5}$$

$A_4 = A_{bol}/(10^4 m^2) \sim 0.1$

$T_s \sim (2-3)MK$

Name	$\hat{P}_3/P$		$L_x/\dot{E}\times 10^{-3}$		$L_x \times 10^{28}$		b	$T_s^{(obs)}$	$T_s^{(pred)}$	B_d	B_s
PSR B	Obs.	Pred.	Obs.	Pred.	Obs.	Pred.	A_{pc}/A_{bol}	10^6 K	10^6 K	10^{12}G	10^{14}G
0943 + 10	37.4	37	$0.5^{+0.2}_{-0.2}$	0.46	5^{+2}_{-2}	4.8	60^{+140}_{-48}	$3.1^{+0.9}_{-1.1}$	3^{+1}_{-1}	3.95	$2.37^{+5.53}_{-1.90}$
1133 + 16	(33^{+3}_{-3})	31^{+3}_{-2}	$0.77^{+0.13}_{-0.18}$	$1.0^{+0.3}_{-0.2}$	$7.7^{+1.3}_{-1.3}$	$8.9^{+1.3}_{-1.8}$	$11.1^{+16.6}_{-5.6}$	$2.8^{+1.2}_{-1.2}$	$2.4^{+0.8}_{-0.5}$	4.25	$0.47^{+0.71}_{-0.24}$
0826 − 34	14^{+1}_{-1}			$3.2^{+0.5}_{-0.4}$		$2.0^{+0.33}_{-0.25}$				2.74	
0834 + 06	15			2.8		37				5.94	

Pulsars are fast rotating and strongly magnetized Neutron Stars (NS)

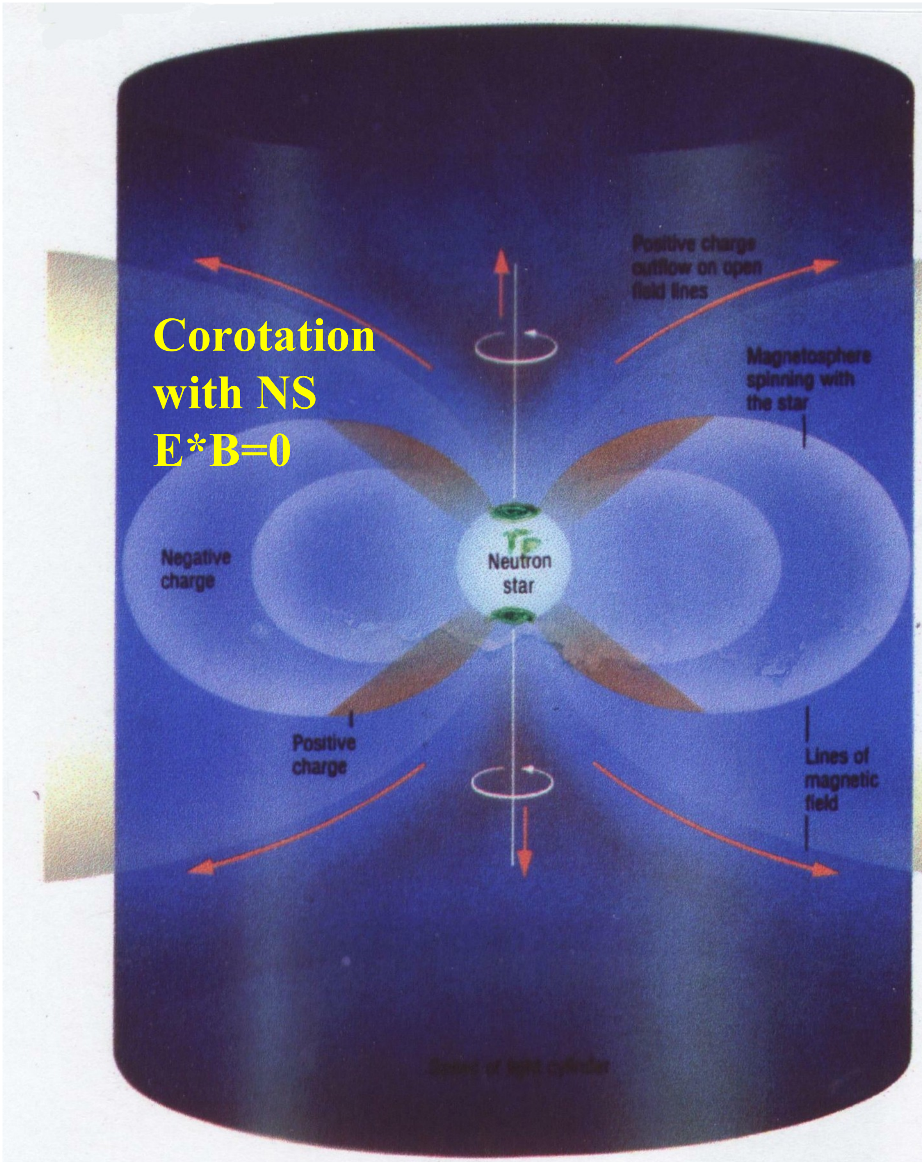

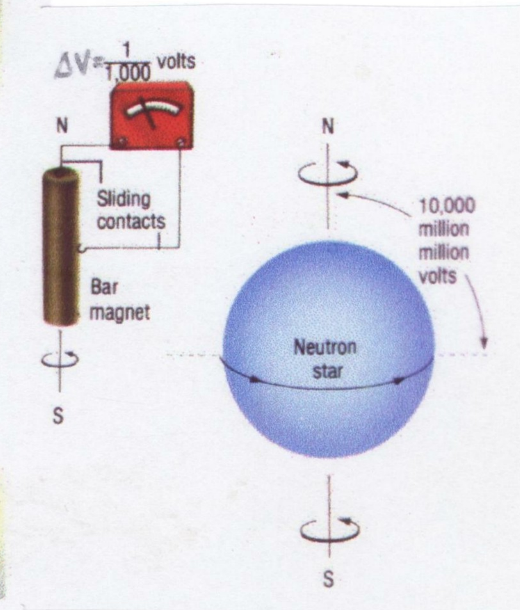

Polar Cap (PC)

region of NS surface connected to ISM via open magnetic field lines penetrating the Light Cylinder

Charged particles will leave through LC due to inertia and create charge depletion just above the PC. If this charge cannot be re-supplied by the PC surface (strong binding) then huge accelerating potential drop will occur along the open magnetic field lines close to the PC surface.

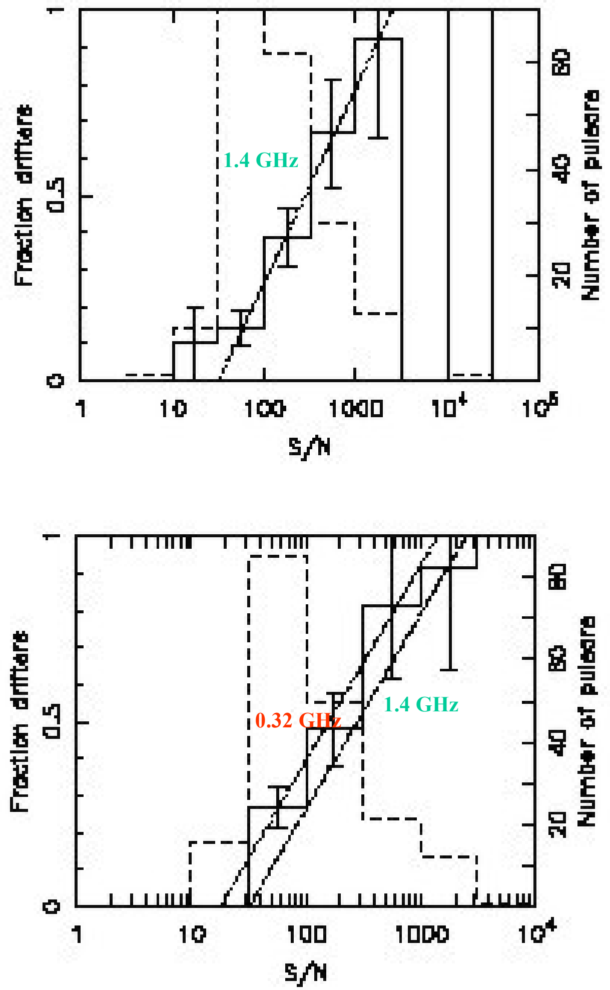

Weltevrede, Edwards & Stappers et al. 2006, 2007